Chapter 1

Intracule Functional Theory

Deborah L. Crittenden and Peter M.W. Gill

Research School of Chemistry,
Australian National University, Canberra ACT 0200, Australia

Density functional theory (DFT) has become the most popular by far of the panoply of methods in quantum chemistry and the reason for this is simple. Where other schemes had become bogged down in mind-numbingly expensive and detailed treatments of the electron correlation problem, DFT simply shrugged, pointed at the Hohenberg–Kohn theorem, and asserted that the correlation energy can be written as an integral of a certain function of the one-electron density. The only thing that irritated the wavefunction people more than the cavalier arrogance of that assertion was the astonishing accuracy of the energies that it yields.

Well, most of the time. Occasionally, DFT fails miserably and, although the reasons for its lapses are now understood rather well, it remains a major challenge to correct these fundamental deficiencies, while retaining the winsome one-electron foundation upon which DFT rests.

Does this mean that, for truly foolproof results, we have no option but to return to the bog of many-body theory? One might think so, at least from a cursory inspection of the current textbooks. But we feel differently, and in this chapter we present an overview of an attractive alternative that lies neither in the one-electron world of DFT, nor in the many-electron world of coupled-cluster theory. Our approach nestles in the *two-electron* "Fertile Crescent" that bridges these extremes, a largely unexplored land that would undoubtedly have been Goldilocks' choice.

We present results that demonstrate that the new approach — Intracule Functional Theory — is capable of predicting the correlation energies of small molecules with an accuracy that rivals that of much more expensive post-Hartree–Fock schemes. We also show that it easily and naturally models van der Waals dispersion energies. However, we also show that

its current versions struggle to capture static correlation energies and that this is an important area for future development.

Finally, we peer into the probable future of the field, speculating on the directions in which we and others are likely to take it. We conclude that, although the approach is conceptually attractive and has shown considerable promise, the investigations hitherto have scarcely scratched the surface and there are ample opportunities for fresh ideas from creative minds.

1.1. Introduction

In the late 1920s, Hartree [1] was among the first to realize that the newly derived Schrödinger equation [2] describing quantum electronic motion could be solved for multi-particle systems if the wavefunction, a complicated multidimensional object that explicitly couples the motion of all particles in the system, is approximated by a product

$$\Psi(\mathbf{r}_1, \mathbf{r}_2, \ldots, \mathbf{r}_n) = \phi_1(\mathbf{r}_1)\phi_2(\mathbf{r}_2)\cdots\phi_n(\mathbf{r}_n) \tag{1.1}$$

of single-particle functions (spin-orbitals). Physically, the Hartree wavefunction implies that each electron moves independently in the electrostatic field created by all of the others. Shortly thereafter, both Slater [3] and Fock [4] pointed out that Hartree's wavefunction lacks the antisymmetry required by the Pauli Principle [5], but that this can be rectified by adopting the determinant form

$$\Psi(\mathbf{r}_1, \mathbf{r}_2, \ldots, \mathbf{r}_n) = \begin{vmatrix} \phi_1(\mathbf{r}_1) & \phi_2(\mathbf{r}_1) & \ldots & \phi_n(\mathbf{r}_1) \\ \phi_1(\mathbf{r}_2) & \phi_2(\mathbf{r}_2) & \ldots & \phi_n(\mathbf{r}_2) \\ \vdots & \vdots & \ddots & \vdots \\ \phi_1(\mathbf{r}_n) & \phi_2(\mathbf{r}_n) & \cdots & \phi_n(\mathbf{r}_n) \end{vmatrix}. \tag{1.2}$$

Unfortunately, the resulting Hartree–Fock (HF) model neglects the interelectron correlations that influence chemically important phenomena such as bond making and breaking, electron gain and loss, and the response of a molecule to an external electric and/or magnetic field. For example, in the homolytic fission of a single bond, the two formerly paired electrons migrate in opposite directions and this cannot be accurately described by a single determinant.

The difference between a molecule's HF energy and its exact energy is E_c, the correlation energy, and the challenge of its determination is known

as the "electron correlation problem" and has been the focus of ongoing research efforts for almost a century. Currently, methods for recovering E_c fall into two broad classes.

Wavefunction-based methods are based upon the mathematical observation that an improved wavefunction can be constructed from the occupied and unoccupied orbitals that arise from solving the HF equations. These methods are guaranteed eventually to converge to the exact result, but their convergence is hampered because they are effectively approximating cusps in the true wavefunction by sums of smooth functions. In practice, wavefunction-based post-HF methods are typically limited in applicability to systems containing a few dozen non-hydrogen atoms.

Density-based methods are a popular low-cost alternative. They are based upon the Hohenberg–Kohn theorem [6], which states that the energy of the ground state of a system is a universal functional of its electron density $\rho(\mathbf{r})$. Unfortunately, the theorem gives little insight into the construction of the functional and, despite the efforts of many researchers over many years, its form remains unknown. Many approximate functionals have been devised, each with its own strengths and weaknesses, but none yet has proven accurate for all types of chemical problems. The major systematic weaknesses [7] of density functional theory (DFT) stem from its inability to deal with intrinsically two-electron phenomena such as bond cleavage and static correlation.

Comparing these two alternatives — wavefunction-based and density-based models — reveals a vast and largely unexplored intermediate ground between the complexity of wavefunction schemes (which depend explicitly on the coordinates of every electron) and the simplicity of density schemes (which depend only on the one-electron density). The most obvious entry point — and this is our present strategy — is to develop approaches that incorporate *two*-electron information but retain the computational advantages enjoyed by DFT. We will use atomic units throughout.

1.2. Intracules

A reasonable starting point for the development of a two-electron analogue of DFT is the two-electron density

$$\rho_2(\mathbf{r}_1, \mathbf{r}_2) = \int |\Psi(\mathbf{r}_1, \ldots, \mathbf{r}_n)|^2 \, d\mathbf{r}_3 \ldots d\mathbf{r}_n, \tag{1.3}$$

which gives the joint probability of finding one electron at $\mathbf{r}_1$ and another at $\mathbf{r}_2$. How might one extract the correlation energy from this six-dimensional object? Intuitively, one may expect the statistical correlation between the motions of two electrons to depend strongly on their separation and this leads naturally to the position intracule [8]

$$P(u) = \int \rho_2(\mathbf{r}_1, \mathbf{r}_2)\delta(r_{12} - u)d\mathbf{r}_1 d\mathbf{r}_2, \tag{1.4}$$

(where δ is the Dirac delta distribution and $r_{12} \equiv |\mathbf{r}_{12}| \equiv |\mathbf{r}_1 - \mathbf{r}_2|$) which gives the probability density of finding two electrons separated by a distance u.

Example 1.1: The Position Intracule for a He-like Ion

In most modern calculations, the molecular orbitals (MOs) are expanded in a basis of Gaussian functions. If we model the $1s$ orbital in a He-like ion by the single Gaussian $\exp(-\alpha r^2)$, the HF wavefunction is

$$\Psi(\mathbf{r}_1, \mathbf{r}_2) = (2\alpha/\pi)^{3/2} \exp[-\alpha(r_1^2 + r_2^2)]$$

and one finds from Eq. (1.4) that the position intracule is

$$\begin{aligned}
P(u) &= \int \rho_2(\mathbf{r}_1, \mathbf{r}_2)\delta(r_{12} - u)d\mathbf{r}_1\, d\mathbf{r}_2 \\
&= (2\alpha/\pi)^3 \int \exp[-2\alpha(r_1^2 + r_2^2)]\delta(r_{12} - u)d\mathbf{r}_1 d\mathbf{r}_2 \\
&= (2\alpha/\pi)^3 \int \exp[-2\alpha(r_1^2 + |\mathbf{r}_1 - \mathbf{u}|^2)]\, d\mathbf{r}_1\, d\Omega_{\mathbf{u}}, \\
&\qquad\qquad \text{by writing } \mathbf{r}_2 = \mathbf{r}_1 - \mathbf{u} \\
&= (\alpha/\pi)^{3/2} \int \exp(-\alpha u^2) d\Omega_{\mathbf{u}}, \\
&\qquad\qquad \text{by integrating over } \mathbf{r}_1 \\
&= (\alpha/\pi)^{3/2} 4\pi u^2 \exp(-\alpha u^2), \quad \text{by integrating over the angular part of } \mathbf{u}
\end{aligned}$$

As the Gaussian exponent α increases, the $1s$ orbital shrinks and $P(u)$ contracts toward the origin.

The Gaussian exponent that minimizes the HF energy of the He atom is $\alpha = \frac{33-8\sqrt{2}}{9\pi}$ and the resulting intracule reveals that the electrons are most likely to be found with a separation $u \approx 1$ but that they are unlikely to be found close to one another ($u \approx 0$) or at large separations ($u > 3$).

Continued

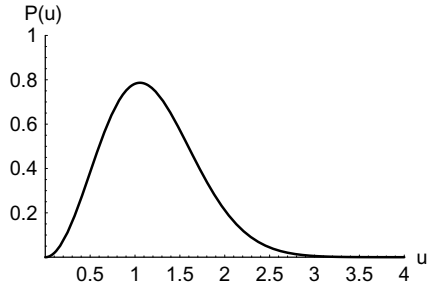

Fig. 1.1. Position intracule for the helium atom.

Unfortunately, although it is easy enough to compute $P(u)$, even in large molecules [9], it is not an optimal source of two-electron information for electron correlation. This can be demonstrated by considering two-electron systems that are confined by a tunable parameter. For example, in the helium-like ions (i.e. H^-, He, $Li^+, \ldots$), where the confinement parameter is the nuclear charge Z, the exact [10] and HF [11] energies are

$$E_{\text{exact}} = -Z^2 + \frac{5}{8}Z - 0.15767 + O(Z^{-1}) \tag{1.5}$$

$$E_{\text{HF}} = -Z^2 + \frac{5}{8}Z - 0.11100 + O(Z^{-1}) \tag{1.6}$$

and therefore, as the confinement parameter grows, the correlation energy $E_c = E_{\text{exact}} - E_{\text{HF}}$ approaches a limiting value ($-46.67\,\text{mE}_\text{h}$). Analogous behaviour is found in other such systems [12] and, indeed, it can be proven [13] that the correlation energy of two electrons always approaches a limiting value when they are confined to an infinitesimal volume. This constancy contrasts sharply with the behaviour of the position intracule $P(u)$, which approaches a delta distribution at $u = 0$ as the two electrons are sequeezed closer together. Such analysis indicates that $P(u)$ does not possess the qualitative behaviour required to capture E_c in these simple systems.

Example 1.2: The Momentum Intracule for a He-like Ion

Modelling the $1s$ orbital in a He-like ion by the Gaussian $\exp(-\alpha r^2)$ yields the HF momentum wavefunction

$$\Phi(\mathbf{p}_1, \mathbf{p}_2) = (2\pi\alpha)^{-3/2} \exp[-(p_1^2 + p_2^2)/4\alpha]$$

Continued

and one finds from Eq. (1.7) that the momentum intracule

$$
\begin{aligned}
M(v) &= \int \pi_2(\mathbf{p}_1, \mathbf{p}_2)\delta(p_{12} - v) d\mathbf{p}_1\, d\mathbf{p}_2 \\
&= (2\pi\alpha)^{-3} \int \exp[-(p_1^2 + p_2^2)/2\alpha]\delta(p_{12} - v) d\mathbf{p_1} d\mathbf{p_2} \\
&= (2\pi\alpha)^{-3} \int \exp[-(p_1^2 + |\mathbf{p}_1 - \mathbf{v}|^2)/2\alpha] d\mathbf{p}_1 d\Omega_{\mathbf{v}}, \\
&\qquad\qquad \text{by writing } \mathbf{p}_2 = \mathbf{p}_1 - \mathbf{v} \\
&= (4\pi\alpha)^{-3/2} \int \exp(-v^2/4\alpha) d\Omega_{\mathbf{v}}, \\
&\qquad\qquad \text{by integrating over } \mathbf{p}_1 \\
&= (4\pi\alpha)^{-3/2} 4\pi v^2 \exp(-v^2/4\alpha), \\
&\qquad\qquad \text{by integrating over the angular part of } \mathbf{v}
\end{aligned}
$$

is a Maxwell distribution. As α increases, high relative momenta become more likely and $M(v)$ broadens.

Using the energy-minimizing exponent $\alpha = \frac{33-8\sqrt{2}}{9\pi}$ yields the momentum intracule which reveals that the electrons are most likely to be moving with a relative momentum $v \approx 2$ but that they are unlikely to have very similar momenta ($v \approx 0$) or very different momenta ($v > 6$).

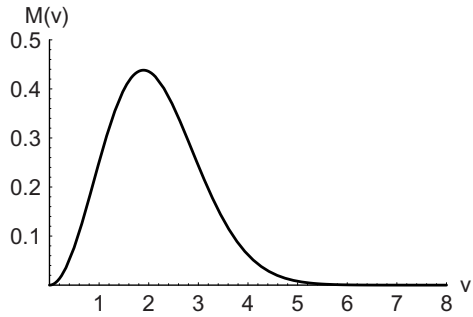

Fig. 1.2. Momentum intracule for the helium atom.

A decade ago, Rassolov observed that the relative momentum $p_{12} \equiv |\mathbf{p}_{12}| \equiv |\mathbf{p}_1 - \mathbf{p}_2|$ also plays a role in electron correlation [14]. Intuitively, this makes sense: high relative velocities reduce interaction times for the

electrons and therefore reduce the extent of their correlation. This information is captured by the momentum intracule [15, 16]

$$M(v) = \int \pi_2(\mathbf{p}_1, \mathbf{p}_2)\delta(p_{12} - v)\, d\mathbf{p}_1 d\mathbf{p}_2, \tag{1.7}$$

where the two-electron momentum density is

$$\pi_2(\mathbf{p}_1, \mathbf{p}_2) = \int |\Phi(\mathbf{p}_1, \ldots, \mathbf{p}_n)|^2 d\mathbf{p}_3 \ldots d\mathbf{p}_n \tag{1.8}$$

and the momentum wavefunction

$$\Phi(\mathbf{p}_1, \ldots, \mathbf{p}_n) = (2\pi)^{-3n/2} \int \Psi(\mathbf{r}_1, \ldots, \mathbf{r}_n) e^{-i(\mathbf{p}_1\cdot\mathbf{r}_1 + \cdots + \mathbf{p}_n\cdot\mathbf{r}_n)} d\mathbf{r}_1 \ldots d\mathbf{r_n} \tag{1.9}$$

is the Fourier transform of the position-space wavefunction. Unfortunately, the momentum intracules of the He-like ions become flatter as Z increases, suggesting that — like $P(u)$ but for the opposite reason — $M(v)$ is not an optimal source of two-electron information for correlation. However, the opposing trends in the position and momentum intracules suggest that we may be able to model correlation through a *product* variable involving both r_{12} and p_{12}.

Yet again, however, it seems that we are thwarted because, although one can form a momentum-space wavefunction from its position-space counterpart using a Fourier transform, the Heisenberg Uncertainty Principle forbids the construction of a *joint* phase-space wavefunction. Likewise, although $\rho_2(\mathbf{r}_1, \mathbf{r}_2)$ and $\pi_2(\mathbf{p}_1, \mathbf{p}_2)$ can be easily obtained, there exists no comparable joint probability density $P(\mathbf{r}_1, \mathbf{r}_2, \mathbf{p}_1, \mathbf{p}_2)$.

Nevertheless, although a genuine density in phase-space is prohibited, it is possible to concoct *quasi*-densities with some of the properties that the genuine article would possess. The most famous of these are the Wigner quasi-densities [17]

$$\begin{aligned} W_n(\mathbf{r}_1, \ldots, \mathbf{r}_n, \mathbf{p}_1, \ldots, \mathbf{p}_n) \\ = \frac{1}{\pi^{3n}} \int \Psi(\mathbf{r}_1 + \mathbf{q}_1, \ldots, \mathbf{r}_n + \mathbf{q}_n)^* \\ \times \Psi(\mathbf{r}_1 - \mathbf{q}_1, \ldots, \mathbf{r}_n - \mathbf{q}_n) e^{2i(\mathbf{p}_1\cdot\mathbf{q}_1 + \cdots + \mathbf{p}_n\cdot\mathbf{q}_n)} d\mathbf{q}_1 \ldots d\mathbf{q}_n \end{aligned} \tag{1.10}$$

and the Husimi quasi-densities [18]. Besley [19] has studied the latter but we will confine our attention here to the former.

Being a function of $6n$ coordinates, the full Wigner quasi-density is even more complicated than the wavefunction. However, because we are

primarily interested in two-electron information, it is natural to integrate over all but two of the electrons to use instead the second-order reduced Wigner quasi-density

$$W_2(\mathbf{r}_1, \mathbf{r}_2, \mathbf{p}_1, \mathbf{p}_2) = \frac{1}{\pi^6} \int \rho_2(\mathbf{r}_1 + \mathbf{q}_1, \mathbf{r}_2 + \mathbf{q}_2, \mathbf{r}_1 - \mathbf{q}_1, \mathbf{r}_2 - \mathbf{q}_2) e^{2i(\mathbf{p}_1 \cdot \mathbf{q}_1 + \mathbf{p}_2 \cdot \mathbf{q}_2)} \, d\mathbf{q}_1 d\mathbf{q}_2, \tag{1.11}$$

where ρ_2 is the reduced second-order density matrix [20]. W_2 is a simpler object than W_n but it is nonetheless a function of 12 variables and is conceptually formidable. Ideally, we would like to extract from it only the information that is directly relevant to a description of electron correlation. It obviously contains information about the relative position r_{12} and momentum p_{12} variables but it also knows about the dynamical angle θ_{12} between the vectors $\mathbf{r}_{12}$ and $\mathbf{p}_{12}$, giving insight into the nature of the electrons' mutual orbit, as illustrated below.

By analogy with Eqs. (1.4) and (1.7), we can extract the quasi-density for r_{12}, p_{12} and θ_{12} to form the Omega intracule [21]

$$\begin{aligned}
&\Omega(u, v, \omega) \\
&= \int W_2(\mathbf{r}_1, \mathbf{r}_2, \mathbf{p}_1, \mathbf{p}_2) \, \delta(r_{12} - u) \, \delta(p_{12} - v) \, \delta(\theta_{12} - \omega) \, d\mathbf{r}_1 \, d\mathbf{r}_2 \, d\mathbf{p}_1 \, d\mathbf{p}_2 \\
&= \frac{1}{\pi^6} \int \rho_2(\mathbf{r}_1 + \mathbf{q}_1, \mathbf{r}_2 + \mathbf{q}_2, \mathbf{r}_1 - \mathbf{q}_1, \mathbf{r}_2 - \mathbf{q}_2) e^{2i(\mathbf{p}_1 \cdot \mathbf{q}_1 + \mathbf{p}_2 \cdot \mathbf{q}_2)} \\
&\quad \times \delta(r_{12} - u) \delta(p_{12} - v) \delta(\theta_{12} - \omega) d\mathbf{q}_1 \, d\mathbf{q}_2 \, d\mathbf{r}_1 \, d\mathbf{r}_2 \, d\mathbf{p}_1 \, d\mathbf{p}_2 \\
&= \frac{1}{8\pi^3} \int \rho_2(\mathbf{r}, \mathbf{r} + \mathbf{q} + \mathbf{u}, \mathbf{r} + \mathbf{q}, \mathbf{r} + \mathbf{u}) e^{i\mathbf{v} \cdot \mathbf{q}} \delta(\theta_{uv} - \omega) \, d\mathbf{r} d\mathbf{q} d\Omega_{\mathbf{u}} d\Omega_{\mathbf{v}},
\end{aligned} \tag{1.12}$$

where, as before, $\mathbf{u}$ and $\mathbf{v}$ are arbitrary vectors of length u and v, respectively, and θ_{uv} is the angle between them. At this point, things do not look very

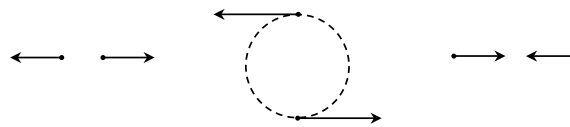

Fig. 1.3. Physical interpretation of the dynamical angle θ_{12}.

practical, for the Omega intracule is written as a ten-dimensional integral over the second-order density matrix. However, as we will see in a moment, things become much more tractable after we introduce a Gaussian basis set.

The Omega intracule is the grandfather of a family of lower-dimensional intracules and each of its descendants is obtained by appropriate integration. This is illustrated diagrammatically below where we also introduce $s = r_{12}p_{12}$ and $x = \mathbf{r}_{12} \cdot \mathbf{p}_{12}$. Both of these variables have dimensions of angular momentum and units of Planck's constant.

If the MOs are expanded in a basis set $\{\phi_i\}$, the reduced second-order density matrix is

$$\rho_2(\mathbf{r}_1, \mathbf{r}_2, \mathbf{r}'_1, \mathbf{r}'_2) = \sum_{abcd} \Gamma_{abcd}\, \phi_a(\mathbf{r}_1)\phi_b(\mathbf{r}_2)\phi_c(\mathbf{r}'_1)\phi_d(\mathbf{r}'_2), \tag{1.13}$$

where the Γ_{abcd} are two-particle density matrix (2PDM) elements. Thus, from Eq. (1.12), the Omega intracule is

$$\Omega(u, v, \omega) = \sum_{abcd} \Gamma_{abcd}\, [abcd]_\Omega, \tag{1.14}$$

where the Omega integrals are

$$[abcd]_\Omega = \frac{1}{8\pi^3} \int \phi_a(\mathbf{r})\phi_b(\mathbf{r}+\mathbf{q}+\mathbf{u})\phi_c(\mathbf{r}+\mathbf{q})\phi_d(\mathbf{r}+\mathbf{u}) \times e^{i\mathbf{v}\cdot\mathbf{q}}\delta(\theta_{uv} - \omega)\, d\mathbf{r}d\mathbf{q}d\Omega_{\mathbf{u}}\, d\Omega_{\mathbf{v}}. \tag{1.15}$$

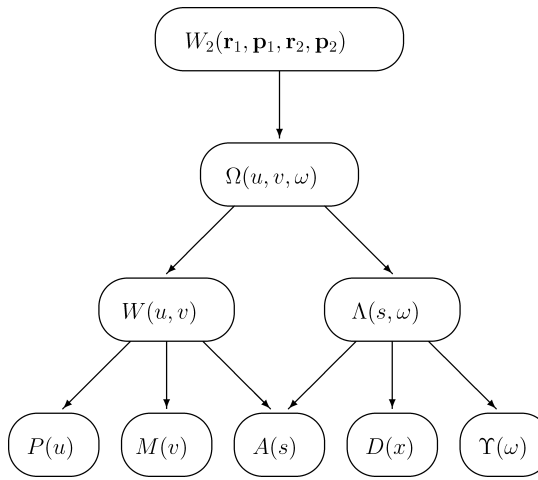

Fig. 1.4. The intracule family tree.

If the ϕ_i are s-type Gaussians centred at **A**, **B**, **C** and **D**, with exponents α, β, γ and δ, it can be shown [22] that

$$[ssss]_\Omega = K \exp(-R) \frac{1}{\pi} \int_0^\pi i_0(\sqrt{x + y\cos t})dt, \tag{1.16}$$

where

$$K = \frac{\pi^2 u^2 v^2 \sin\omega}{(\alpha+\delta)^{3/2}(\beta+\gamma)^{3/2}} \exp(-\lambda^2 u^2 - \mu^2 v^2 - i\eta u v \cos\omega) \tag{1.17}$$

$$R = \frac{\alpha\delta}{\alpha+\delta}|\mathbf{A}-\mathbf{D}|^2 + \frac{\beta\gamma}{\beta+\gamma}|\mathbf{B}-\mathbf{C}|^2 \tag{1.18}$$

$$\begin{aligned} x &= (Pu)^2 + (iQv)^2 + 2(Pu)(iQv)\cos\chi\cos\omega \\ y &= 2(Pu)(iQv)\sin\chi\sin\omega \end{aligned} \tag{1.19}$$

$$\lambda^2 = \frac{\alpha\delta}{\alpha+\delta} + \frac{\beta\gamma}{\beta+\gamma} \quad 4\mu^2 = \frac{1}{\alpha+\delta} + \frac{1}{\beta+\gamma} \quad \eta = \frac{\alpha}{\alpha+\delta} - \frac{\beta}{\beta+\gamma} \tag{1.20}$$

$$\begin{aligned} \mathbf{P} &= \frac{2\alpha\delta}{\alpha+\delta}(\mathbf{A}-\mathbf{D}) + \frac{2\beta\gamma}{\beta+\gamma}(\mathbf{B}-\mathbf{C}) \\ \mathbf{Q} &= \frac{\alpha\mathbf{A}+\delta\mathbf{D}}{\alpha+\delta} - \frac{\beta\mathbf{B}+\gamma\mathbf{C}}{\beta+\gamma} \quad \mathbf{P}\cdot\mathbf{Q} = PQ\cos\chi \end{aligned} \tag{1.21}$$

and $i_0(z) = z^{-1}\sinh z$. The integral in Eq. (1.16) can be evaluated by quadrature or series expansion [22]. However, if the Gaussian centres are collinear, it can be found in closed form and, if they are concentric, it reduces to

$$[ssss]_\Omega = K. \tag{1.22}$$

Integrals over the p, d, ... basis functions may be obtained by systematic Boys differentiation [23] of the $[ssss]_\Omega$ integral. However, it is more efficient to use recursion and a 18-term recurrence relation has been developed for this purpose [24].

Example 1.3: The Intracule Family for a He-like Ion

As in the previous examples, the HF wavefunction of a He-like ion in the basis of a single Gaussian is

$$\Psi(\mathbf{r}_1, \mathbf{r}_2) = (2\alpha/\pi)^{3/2} \exp[-\alpha(r_1^2 + r_2^2)]$$

and one finds from Eq. (1.22) that the Omega intracule is

$$\Omega(u, v, \omega) = (1/\pi)u^2 \exp(-\alpha u^2)\, v^2 \exp(-v^2/4\alpha) \sin\omega.$$

Continued

In this simple system, we find that $\Omega(u, v, \omega)$ is proportional to the product of $P(u)$ and $M(v)$, implying that u and v are statistically independent. However, such systems are the exception, not the rule.

The lower intracules can be constructed easily from $\Omega(u, v, \omega)$, as shown below:

Intracule	Construction	Explicit form
$W(u, v)$	$\int_0^\pi \Omega(u, v, \omega) d\omega$	$(2/\pi)u^2 \exp(-\alpha u^2) v^2 \exp(-v^2/4\alpha)$
$\Lambda(s, \omega)$	$\int_0^\infty \Omega(u, s/u, \omega) u^{-1} du$	$(1/\pi)s^2 K_0(s) \sin\omega$
$P(u)$	$\int_0^\infty W(u, v) dv$	$(\alpha/\pi)^{3/2} 4\pi u^2 \exp(-\alpha u^2)$
$M(v)$	$\int_0^\infty W(u, v) du$	$(4\pi\alpha)^{-3/2} 4\pi v^2 \exp(-v^2/4\alpha)$
$A(s)$	$\int_0^\pi \Lambda(s, \omega) d\omega$	$(2/\pi)s^2 K_0(s)$
$D(x)$	$\int_x^\infty \Lambda(s, \omega)(s \sin\omega)^{-1} ds$	$(1/\pi)x K_1(x)$
$\Upsilon(\omega)$	$\int_0^\infty \Lambda(s, \omega) ds$	$(1/2)\sin\omega$

Here K_0 and K_1 are modified Bessel functions of the second kind [25].

Each of the three one-dimensional intracules, $A(s)$, $D(x)$ and $\Upsilon(\omega)$, whose graphs are shown below, is independent of the exponent α, that is, they are invariant with respect to dilation. As such, they apply not only to the helium atom but, equally, to any helium-like ion. This will be important in Section 1.3.

The attentive reader may wonder why, if u and v are statistically independent in this system, the angle intracule $\Upsilon(\omega)$ is not constant. After all, if the relative positions and momenta of the two electrons are independent, one might have expected the angle between $\mathbf{r}_{12}$ and $\mathbf{p}_{12}$ to be equally likely to take any value between 0 and π. The fact that this is not the case is a purely geometrical ("Jacobian") effect: as $\mathbf{r}_{12}$ and $\mathbf{p}_{12}$ range independently over their respective domains, dynamical angles θ_{12} close to $\pi/2$ arise far more often than angles close to 0 or π. The fact that there are many more points on the Earth's surface with latitudes near 0° (equatorial regions) than with latitudes near 90° (polar regions) arises from the same geometrical effect.

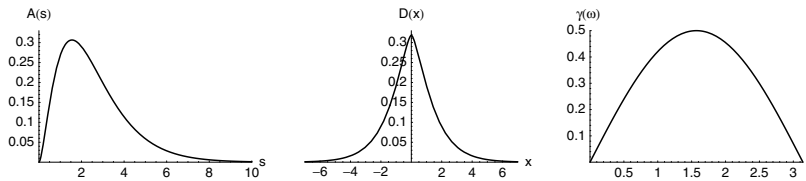

Fig. 1.5. Action, dot and angle intracules for a He-like ion.

Example 1.4: The Wigner Intracule for the Be Atom

The STO–3G basis for the Be atom consists of two three-fold contracted Gaussian-type functions. Total contraction coefficient arrays for the 1*s* and 2*s* molecular orbitals ($\mathbf{C}^1$ and $\mathbf{C}^2$, respectively) are calculated by multiplying the normalized contraction coefficients by the appropriate MO coefficients.

Index	Gaussian exponent	Contraction coefficient	1*s* MO coefficient	2*s* MO coefficient	1*s* array $\mathbf{C}^1$	2*s* array $\mathbf{C}^2$
1	30.167871	1.4158460			1.4057909	−0.4160898
2	5.495115	1.3693446	0.9928982	−0.2938807	1.3596198	−0.4024239
3	1.487193	0.4267649			0.4237341	−0.1254180
4	1.3148331	−0.08747241			−0.0022866	−0.0905572
5	0.3055389	0.11701478	0.0261377	1.0351471	0.0030585	0.1211275
6	0.09937070	0.088312776			0.0023083	0.0914167

The HF two-particle density matrix elements can be constructed using

$$\Gamma_{abcd} = C_a^1 C_b^1 C_c^1 C_d^1 + 4C_a^1 C_b^1 C_c^2 C_d^2 + C_a^2 C_b^2 C_c^2 C_d^2 - 2C_a^1 C_b^2 C_c^2 C_d^1,$$

where C_a^k denotes the ath element of the $\mathbf{C}^k$ array. The Wigner intracule is then assembled through

$$W(u, v) = \sum_{a=1}^{6} \sum_{b=1}^{6} \sum_{c=1}^{6} \sum_{d=1}^{6} \Gamma_{abcd}\, [abcd]_W$$

and it is illustrated in the following contour plot:

This intracule possesses three maxima. The first, near $(u, v) \approx (0.7, 3)$, describes electrons that are close together and moving fast; it arises from observing the two 1*s* electrons. The second, near $(u, v) \approx (2.5, 0.8)$, describes electrons that are well-separated and moving relatively slowly; it arises from observing the two 2*s* electrons. The third, near $(u, v) \approx (2, 2)$, describes electrons that are moderately far apart and moving at a moderate pace; it arises from observing a 1*s* electron and a 2*s* electron. The third maximum is the largest because there are ${}_4C_2 = 6$ ways to choose two of the electrons, and four of these choices involve a 1*s* and a 2*s* electron.

Continued

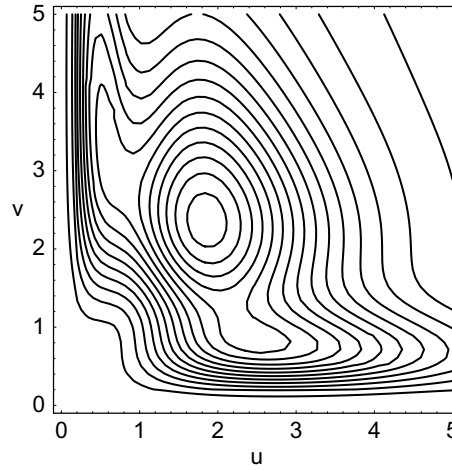

Fig. 1.6. Wigner intracule for the beryllium atom.

1.3. Electron Correlation Models

The Omega intracule for an atomic or molecular system provides an impressively detailed picture of the dynamical behaviour of its electrons. We know, for any given values of u, v and ω, the (quasi-)probability of finding two of its electrons at a distance u, moving with a relative speed v at a dynamical angle ω. This now allows us to return to our original question: can we exploit this information to predict electron correlation energies?

The foundation of DFT methods is the Hohenberg–Kohn theorem [6], which assures us that the correlation energy is a functional of the one-electron density $\rho(\mathbf{r})$. We now make an analogous conjecture [21]: that the correlation energy is a functional of the Omega intracule, i.e.

$$E_c = F[\Omega(u, v, \omega)]. \tag{1.23}$$

To prove this remains an interesting open challenge and there are surely many possible lines of attack. Our earliest attempts sought to show that the Hamiltonian can be reconstructed (apart from unimportant translations and rotations) from the intracule. If this can be shown, it proves the conjecture, for the correlation energy is certainly a functional of the Hamiltonian. However, even in the absence of a proof, we feel that the correlation-relevant information in the Omega intracule is much more *accessible* than that in the one-electron density and, therefore, it should be easier to recover

E_c from $\Omega(u, v, \omega)$ than from $\rho(\mathbf{r})$. We call this idea Intracule Functional Theory (IFT).

Although one can imagine many ways to extract E_c from $\Omega(u, v, \omega)$, one of the simplest is to contract the intracule with an appropriate kernel, writing

$$E_c = \int_0^\infty \int_0^\infty \int_0^\pi \Omega(u, v, \omega) G(u, v, \omega) d\omega dv du. \tag{1.24}$$

In such a formulation, the correlation kernel $G(u, v, \omega)$ acts as a weighting function, assigning high priority to regions of intracule space where the electrons are strongly correlated, and low priority to regions where correlation is weak. The thought experiment summarized in the diagram below helps to guide our thinking about this. In situations where both u and v are small, the electrons are close together and moving relatively slowly and so we anticipate a large correlation contribution. Conversely, correlation effects should be small when the electrons are far apart and moving quickly. In intermediate cases, where one of u and v is large and the other is small, we expect moderate correlation effects. This picture fits nicely with the conclusion in the preceding section that correlation in the He-like ions depends in some way on the product $r_{12} p_{12}$.

If the wavefunction is expanded in a Gaussian basis, then combining Eqs. (1.14) and (1.24) yields

$$E_c = \sum_{abcd} \Gamma_{abcd} \, [abcd]_G \tag{1.25}$$

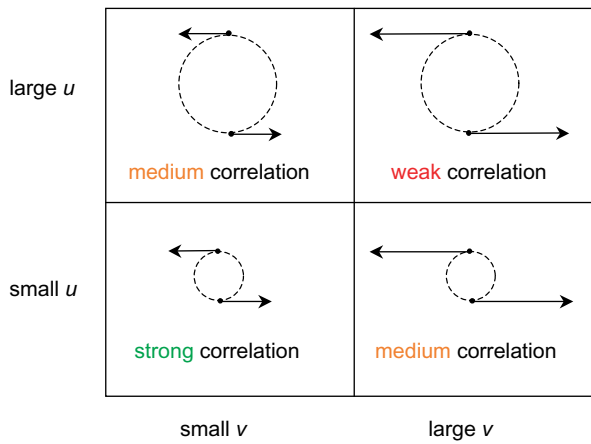

Fig. 1.7. Four interaction scenarios for two electrons.

and it can be shown that the correlation integrals are given by

$$[abcd]_G = \frac{1}{8(\alpha+\delta)^{3/2}(\beta+\gamma)^{3/2}} \times \int \exp(-\lambda^2 u^2 - \mu^2 v^2 - i\eta \mathbf{u}\cdot\mathbf{v} - \mathbf{P}\cdot\mathbf{u} - i\mathbf{Q}\cdot\mathbf{v} - R) \times G(u, v, \omega)\, d\mathbf{u}\, d\mathbf{v}. \tag{1.26}$$

The four-parameter generalized Gaussian kernel [26]

$$G_4(u, v, \omega) = c \exp(-\lambda_0^2 u^2 - \mu_0^2 v^2 - i\eta_0 uv \cos\omega) \tag{1.27}$$

has the attractive property that it leads to correlation integrals that can be found in closed form. For example,

$$[ssss]_G = c\frac{\pi^3}{(\alpha+\delta)^{3/2}(\beta+\gamma)^{3/2}(4l^2m^2+h^2)^{3/2}} \times \exp\left[\frac{m^2P^2 + hPQ\cos\chi - l^2Q^2}{4l^2m^2+h^2} - R\right]. \tag{1.28}$$

where $l^2 = \lambda^2 + \lambda_0^2$, $m^2 = \mu^2 + \mu_0^2$ and $h = \eta + \eta_0$. Except where otherwise indicated, the numerical results below use this kernel with two-particle density matrices Γ_{abcd} from (spin-unrestricted) UHF/6-311G wavefunctions.

Optimization of the parameters (c, η_0, λ_0 and μ_0) in the G_4 kernel against the exact correlation energies [27] of the ground states of the first 18 atoms [28, 29] and the 56 small molecules in Pople's G_1 data set [30] revealed that, whereas η_0 plays a critical role in capturing the correlation energies in these systems, μ_0 is unimportant and can be set to zero without affecting the results significantly. Accordingly, we optimized and explored the two simpler kernels

$$G_2(u, v, \omega) = c \exp(-i\eta_0 uv \cos\omega) \quad (c = 0.07695, \eta_0 = 0.8474) \tag{1.29}$$

$$G_3(u, v, \omega) = c \exp(-\lambda_0^2 u^2 - i\eta_0 uv \cos\omega) \quad (c = 0.2113, \eta_0 = 1.0374, \lambda_0 = 0.5578) \tag{1.30}$$

The correlation energies predicted by the G_2 and G_3 kernels (denoted E_c^2 and E_c^3, respectively) are plotted below against the exact correlation energies of the 18 atoms and 56 molecules described above.

The first thing that one learns from these scatterplots is that these simple kernels are surprisingly successful at capturing the principal correlation effects in these 74 systems. It is very encouraging to find that the G_2

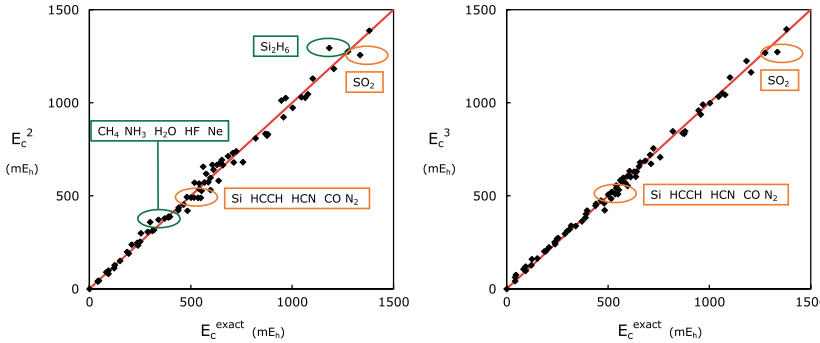

Fig. 1.8. Comparison of correlation energies from the G_2 kernel (left) and G_3 kernel (right) with exact correlation energies.

kernel — which is simply an exponential in $x = \mathbf{r}_{12} \cdot \mathbf{p}_{12}$ — performs so well. On closer inspection, we see that the G_2 kernel tends to overestimate E_c in σ-bonded molecules such as CH_4 and Si_2H_6 and to underestimate in π-bonded molecules such as N_2 and HCCH. The overestimation in the σ-bonded systems is substantially reduced by the G_3 kernel, whose extra $\exp(-\lambda_0^2 u^2)$ factor decreases the predicted correlation energies in spatially extended systems. However, even the G_3 kernel still underestimates E_c in compact, π-bonded molecules.

Why are the unsaturated molecules problematic? It appears that it is because a significant fraction of E_c in these systems is "static," rather than "dynamic," in nature. Though precise definitions are elusive, static correlation is associated with the presence of low-lying excited states and the resulting inadequacy of a single determinant wavefunction, whereas dynamic correlation results from the intricate dance of the electrons as they strive to avoid close encounters with one another. Evidently, our G_2 and G_3 correlation models are effective at modelling dynamical correlation but struggle to capture the static component.

1.4. Dynamic and Static Correlation

The total correlation energy, which is defined [31] as the difference

$$E_c = E_{\text{exact}} - E_{\text{UHF/CBS}} \tag{1.31}$$

between the exact and UHF energies at the complete basis set (CBS) limit, can be partitioned into a static part

$$E_{\text{stat}} = E_{\text{CASSCF(val)/CBS}} - E_{\text{UHF/CBS}} \tag{1.32}$$

and a dynamic part

$$E_{\mathrm{dyn}} = E_{\mathrm{exact}} - E_{\mathrm{CASSCF(val)/CBS}} \tag{1.33}$$

where CASSCF(val) refers to the Complete Active Space SCF method [32] within a full-valence active space. Although this partition is just one of many that have been suggested, it has the twin virtues of conceptual simplicity and computational tractability, at least for smallish systems.

One of the simplest and most instructive systems in which both E_{stat} and E_{dyn} are significant is partially dissociated H_2 and the graph below shows how E_c (solid black), E_{dyn} (dashed black [33]), and E_c^3 (solid grey, from Eq. (1.30)) evolve as the bond length R varies from 0.2 to 3.8 Å. The cusp in the E_{dyn} curve arises from the well-known RHF $\rightarrow$ UHF instability around 1.2 Ångstrom. It is clear that the E_c^3 model reproduces the behaviour of E_c poorly, but that it bears some similarity to the E_{dyn} curve. This confirms our earlier observation that our simple IFT models capture primarily dynamic, rather than static, correlation energy.

If we re-fit the G_3 kernel to the E_{dyn} curve, we obtain the new parameters $c = 0.090$, $\eta_0 = 0.85$ and $\lambda_0 = 0.525$ and the resulting E_{dyn}^3 energies (dashed grey) match E_{dyn} with near-mE_h accuracy. Continuing in this vein, we can abandon the HF/6-311G two-particle density matrix in favour of the CASSCF(val)/6-311G one and, by re-fitting the G_3 kernel again, we obtain the parameters $c = 0.102$, $\eta_0 = 1.02$, $\lambda_0 = 0.43$. The resulting energies match E_{dyn} with sub-mE_h accuracy at all bond lengths. This suggests that combining an IFT-based treatment of dynamic correlation with a full-valence multireference method will produce a method that is capable of estimating E_c very accurately.

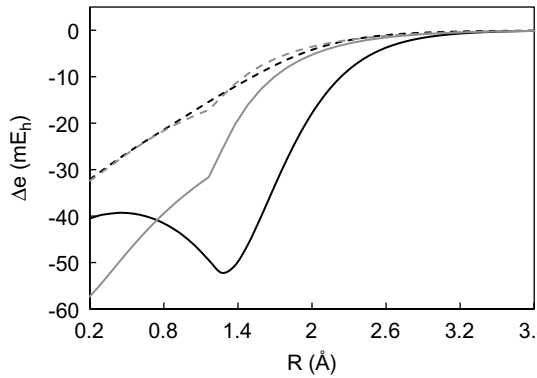

Fig. 1.9. Correlation energy in the H_2 molecule as a function of bond length.

Of course, multireference methods are exponentially expensive, but a hierarchy of approximations can be constructed to reduce the computational cost of this step [34]. Furthermore, the Density Matrix Renormalization Group method (see Chapter 3) provides an alternate route to obtaining static correlation energies and, in some cases, it dramatically outperforms conventional wavefunction methods.

Although the absolute error in the IFT dynamic correlation energy is small everywhere, its *relative* error grows exponentially with R. This is because, whereas the correlation energy from any kernel of the form (1.30) decays exponentially with R, the true E_c decays as R^{-6}. Accordingly, we now turn our attention to London dispersion.

1.5. Dispersion Energies

London Model of Dispersion Energy

The Hamiltonian for two Coulomb-coupled oscillators with force constant $k = 4\alpha^2$, separated by $\mathbf{R}$, is

$$\hat{H} = -\frac{\nabla_1^2 + \nabla_2^2}{2} + 2\alpha^2(r_1^2 + r_2^2) + \frac{1}{|\mathbf{R}|} - \frac{1}{|\mathbf{R} + \mathbf{r}_1|} - \frac{1}{|\mathbf{R} - \mathbf{r}_2|} + \frac{1}{|\mathbf{R} + \mathbf{r}_1 - \mathbf{r}_2|}.$$

If $R \gg 1$, the sum of the Coulomb interactions is dominated by the dipole-dipole term and we can write

$$\hat{H}' = -\frac{\nabla_1^2 + \nabla_2^2}{2} + 2\alpha^2(r_1^2 + r_2^2) + \frac{x_1x_2 + y_1y_2 - 2z_1z_2}{R^3}.$$

If we transform to extracule and intracule coordinates, i.e.

$$\mathbf{S} = \frac{\mathbf{r}_1 + \mathbf{r}_2}{\sqrt{2}} \quad \mathbf{T} = \frac{\mathbf{r}_1 - \mathbf{r}_2}{\sqrt{2}},$$

then $\hat{H}'$ becomes fully separable and its lowest eigenvalue is

$$E = 2\sqrt{\alpha^2 + \frac{1}{4R^3}} + 2\sqrt{\alpha^2 - \frac{1}{4R^3}} + \sqrt{\alpha^2 - \frac{1}{2R^3}} + \sqrt{\alpha^2 + \frac{1}{2R^3}}.$$

Because R is large, we can expand E as a power series in $1/R$ to obtain

$$E = 6\alpha - \frac{3}{32\alpha^3 R^6} + \cdots$$

and subtracting the energy of the uncoupled oscillators yields the celebrated London dispersion energy

$$E_c \sim -\frac{3}{32\alpha^3 R^6}.$$

At large bond lengths ($R \gg 5$ Å), the UHF energy of H_2 rapidly approaches the energy of two non-interacting H atoms and fails to capture the long-range dynamic correlation that is responsible for the weak van der Waals attraction. This long-range correlation energy can be rationalized by considering a multipole expansion of the Coulomb operator, as pioneered by London in the early 1930s [35, 36].

Can we use IFT to model dispersion? To answer this, we begin by considering the simple system — two Coulomb-coupled harmonic oscillators — that London used to model dispersion effects. He showed that its dispersion energy is asymptotically $E_c \sim -3/(32\alpha^3 R^6)$ and his derivation is outlined in the box above. Therefore, we must devise kernels that recover this asymptotic dispersion energy from this system's intracules. Because we favour kernels that depend on $x = \mathbf{r}_{12} \cdot \mathbf{p}_{12}$, we confine our attention to the $D(x)$ intracule and seek kernels that satisfy

$$E_c \sim \int_{-\infty}^{\infty} D(x)G(x)dx. \tag{1.34}$$

or equivalently, by Parseval's Theorem,

$$E_c \sim \int_{-\infty}^{\infty} \hat{D}(k)\hat{G}(k)dk. \tag{1.35}$$

where the hats indicate Fourier transforms.

Example 1.6: The Intracule Family for the H$\cdots$H Complex

The UHF wavefunction for very stretched H$\cdots$H in a single-Gaussian basis is

$$\Psi(\mathbf{r}_1, \mathbf{r}_2) = (2\alpha/\pi)^{3/2} \exp[-\alpha(|\mathbf{r}_1 - \mathbf{R}/2|^2 + |\mathbf{r}_2 + \mathbf{R}/2|^2)]$$

and one finds from Eq. (1.16) that the Omega intracule is

$$\Omega(u, v, \omega) = (1/\pi)u^2 \exp[-\alpha(u^2 + R^2)]i_0(2\alpha Ru)v^2 \exp(-v^2/4\alpha) \sin\omega.$$

By integrating appropriately, we can find some of the lower intracules in closed form, *viz.*

$$\begin{aligned} W(u, v) &= (2/\pi)u^2 \exp[-\alpha(u^2 + R^2)]i_0(2\alpha Ru)v^2 \exp(-v^2/4\alpha) \\ P(u) &= (\alpha/\pi)^{3/2} 4\pi u^2 \exp[-\alpha(u^2 + R^2)]i_0(2\alpha Ru) \\ M(v) &= (4\pi\alpha)^{-3/2} 4\pi v^2 \exp(-v^2/4\alpha) \\ \Upsilon(\omega) &= (1/2)\sin\omega \end{aligned}$$

Continued

and the others in their Fourier representation, *viz.*

$$\Lambda(s,\omega) = \frac{s^2 \sin\omega}{\pi} \int_0^\infty \frac{k^2 j_0(ks)}{(1+k^2)^{3/2}} \exp\left(-\frac{\alpha R^2 k^2}{1+k^2}\right) dk$$

$$A(s) = \frac{2s^2}{\pi} \int_0^\infty \frac{k^2 j_0(ks)}{(1+k^2)^{3/2}} \exp\left(-\frac{\alpha R^2 k^2}{1+k^2}\right) dk$$

$$D(x) = \frac{1}{2\pi} \int_{-\infty}^\infty \frac{\cos kx}{(1+k^2)^{3/2}} \exp\left(-\frac{\alpha R^2 k^2}{1+k^2}\right) dk,$$

where $j_0(z) = z^{-1}\sin z$. We note that the Omega intracule, and therefore all the lower intracules, are non-negative everywhere. As $R \to 0$, they reduce to the intracules of the He-like ions (see Example 1.3).

Fortunately, all of the intracules (or their Fourier transforms) of London's model can be found in closed form and they are shown in Example 1.5. By combining Eq. (1.35) with the expression for $D(x)$, we find that we require

$$\int_{-\infty}^\infty \frac{\hat{G}(k)}{(1+k^2)^{3/2}} \exp\left(-\frac{T^2 k^2}{1+k^2}\right) dk \sim -\frac{3}{32T^6}, \tag{1.36}$$

where $T = \sqrt{\alpha}R$ is large. It is not difficult to show that Eq. (1.36) is satisfied by any kernel of the form

$$\hat{G}(k) \sim -\frac{3}{64}|k|^5 g(k), \tag{1.37}$$

where $g(k)$ is an even function with $g(0) = 1$ and $g(\pm\infty) = 0$. An obvious example of this is

$$\hat{G}(k) = -\frac{3}{64}|k|^5 \exp(-\zeta|k|) \Longrightarrow G(x) = \frac{45}{8}\left[(x+i\zeta)^{-6} + (x-i\zeta)^{-6}\right]. \tag{1.38}$$

By construction, a dispersion kernel $G(x)$ such as the one in Eq. (1.38) is guaranteed (for any ζ) to yield the correct asymptotic dispersion energy when applied to London's system of harmonic oscillators. But does it provide us with a useful dispersion model when applied to chemical systems? To begin to answer this question, one should apply it to pairs of small atoms whose C_6 dispersion coefficients (i.e. coefficients of R^{-6}) are known accurately from experiment or high-level theory. We have done this [37], using the UHF/6-311G density matrices of the H, He, Li and Be atoms, and the results are shown in Table 1.1 below. Given that the exact

Table 1.1. C_6 dispersion coefficients (in atomic units) for pairs of small atoms.

	Exact values				From Eq. (1.38)			
	H	He	Li	Be	H	He	Li	Be
H	6.5				12.2			
He	2.8	1.5			5.2	3.3		
Li	66.5	22.5	1395		74.2	17.2	1534	
Be	34.8	13.2	478	213	76.6	23.0	847	657

C_6 coefficients range over three orders of magnitude, the discovery that the IFT estimates are usually accurate to within a factor of two is a promising start. Once again, this demonstrates the fundamental suitability of IFT for capturing intrinsically two-electron correlation effects.

1.6. Future Prospects

In the teething stages of the development of DFT, much progress was made through a primarily empirical approach. Indeed, between Slater's introduction of Xα theory [38] in 1951 and the publication of the Hohenberg–Kohn theorem [6] 13 years later, it was not even realized that DFT was a theoretically justifiable theory: rather, it was embraced simply because it was a model that worked, surprisingly often.

In some ways, contemporary IFT has evolved similarly, and now stands at a similar point. It is clearly capable of yielding chemically useful quantitative predictions but, for the moment, it lacks the solid foundation of a Hohenberg–Kohn analogue. This deficiency may deter the purist, but the pragmatist finds it difficult to resist the allure of a model that seeks to rationalize the correlation phenomenon through a simple, quasi-classical two-electron picture.

So, what are the likely directions for the development of IFT in the near future?

As functional manufacture has become an industry within DFT, we foresee the construction of new and improved kernels as one of the most obvious threads of future IFT research. To ensure that this progress is rational, we expect that properties of the "exact kernel" will also be derived and that these will be used as guides.

However, we also foresee the real possibility that the kernel ansatz (1.24) may be obsolesced by the discovery of alternative methods for extracting

E_c from the Omega intracule. Perhaps such methods will be found as by-products of the construction of a rigorous proof of the central IFT conjecture (1.23).

Of course, it is also possible that the Omega intracule family tree does not contain the "ultimate" intracule and that, in the future, it will be replaced by a different, and quantum mechanically rigorous, family. We are optimistic about this because it has been shown recently that the Dot intracule $D(x)$ is actually a first-order (in $\hbar$) approximation to the true density of the x variable. Furthermore, the exact density $X(x)$ has also been discovered [39–41] and it is no more difficult to extract from the wavefunction than is $D(x)$.

Finally, we conclude with a statement that is surpassingly obvious and yet often overlooked. If we are to refine and enrich our understanding of the electron correlation phenomenon, we must continue to unearth and analyze simple systems where the phenomenon is most clearly exposed and most readily comprehended. The helium atom, the hydrogen molecule and the uniform electron gas have all proven to be rich veins in the past but our quest for deeper understanding must be an ongoing one and there is no doubt whatever that there is much to be learned from other prototypical systems [42].

Bibliography

[1] D.R. Hartree, *Proc. Cam. Phil. Soc.* **24**, 89 (1928).
[2] E. Schrodinger, *Ann. Phys.* **79**, 361 (1926).
[3] J.C. Slater, *Phys. Rev.* **34**, 1293 (1929).
[4] V. Fock, *Z. Physik.* **61**, 126 (1930).
[5] W. Pauli, *Z. Physik.* **31**, 765 (1925).
[6] P. Hohenberg and W. Kohn, *Phys. Rev. B* **136**, 864 (1964).
[7] A.J. Cohen, P. Mori-Sanchez, and W. Yang, *Science* **321**, 792 (2008).
[8] C.A. Coulson and A.H. Neilson, *Proc. Phys. Soc.* (*London*) **78**, 831 (1961).
[9] A.M. Lee and P.M.W. Gill, *Chem. Phys. Lett.* **313**, 271 (1999).
[10] J.D. Baker, D.E. Freund, R. Nyden Hill, and J.D. Morgan III, *Phys. Rev. A* **41**, 1247 (1990).
[11] J. Linderberg, *Phys. Rev.* **121**, 816 (1961).
[12] P.F. Loos and P.M.W. Gill, *J. Chem. Phys.* **131**, 241101 (2009).
[13] P.F. Loos and P.M.W. Gill, *Phys. Rev. Lett.* **105**, 113001 (2010).
[14] V.A. Rassolov, *J. Chem. Phys.* **110**, 3672 (1999).
[15] K.E. Banyard and C.E. Reed, *J. Phys. B* **11**, 2957 (1978).
[16] N.A. Besley, A.M. Lee, and P.M.W. Gill, *Mol. Phys.* **100**, 1763 (2002).
[17] E. Wigner, *Phys. Rev.* **40**, 749 (1932).
[18] K. Husimi, *Proc. Phys. Math. Soc. Japan* **22**, 264 (1940).

[19] N.A. Besley, *Chem. Phys. Lett.* **409**, 63 (2005).
[20] E.R. Davidson, *Reduced Density Matrices in Quantum Chemistry* (Academic, New York, 1976).
[21] P.M.W. Gill, D.L. Crittenden, D.P. O'Neill, and N.A. Besley, *Phys. Chem. Chem. Phys.* **8**, 15 (2006).
[22] D.L. Crittenden and P.M.W. Gill, *J. Chem. Phys.* **127**, 014101 (2007).
[23] S.F. Boys, *Proc. Roy. Soc.* (*London*) **A200**, 542 (1950).
[24] J.W. Hollett and P.M.W. Gill, *Phys. Chem. Chem. Phys.* **13**, 2972 (2011).
[25] *NIST handbook of mathematical functions*, edited by F.W.J. Olver, D.W. Lozier, R.F. Boisvert, and C.W. Clark (Cambridge University Press, New York, 2010).
[26] D.L. Crittenden, E.E. Dumont, and P.M.W. Gill, *J. Chem. Phys.* **127**, 141103 (2007).
[27] D.P. O'Neill and P.M.W. Gill, *Mol. Phys.* **103**, 763 (2005).
[28] E.R. Davidson, S.A. Hagstrom, S.J. Chakravorty, V. Meiser Umar, and C. Froese Fischer, *Phys. Rev. A* **44**, 7071 (1991).
[29] S.J. Chakravorty, S.R. Gwaltney, E.R. Davidson, F.A. Parpia, and C. Froese Fischer, *Phys. Rev. A* **47**, 3649 (1993).
[30] J.A. Pople, M. Head-Gordon, D.J. Fox, K. Raghavachari, and L.A. Curtiss, *J. Chem. Phys.* **90**, 5622 (1989).
[31] J.A. Pople and J.S. Binkley, *Mol. Phys.* **29**, 599 (1975).
[32] B.O. Roos and P.R. Taylor, *Chem. Phys.* **48**, 157 (1980).
[33] V.A. Rassolov, M.A. Ratner, and J.A. Pople, *J. Chem. Phys.* **112**, 4014 (2000).
[34] D.L. Crittenden and P.M.W. Gill, to be published.
[35] F. London, *Z. Physik. Chem. B* **11**, 222 (1930).
[36] F. London, *Trans. Faraday. Soc.* **33**, 8 (1937).
[37] D.L. Crittenden, P. Xu, and P.M.W. Gill, to be published.
[38] J.C. Slater, *Phys. Rev.* **81**, 385 (1951).
[39] Y.A. Bernard and P.M.W. Gill, *New J. Phys.* **11**, 083015 (2009).
[40] Y.A. Bernard and P.M.W. Gill, *J. Phys. Chem. Lett.* **1**, 1254 (2010).
[41] Y.A. Bernard, D.L. Crittenden and P.M.W. Gill, *J. Phys. Chem. A* **114**, 11984 (2010).
[42] P.F. Loos and P.M.W. Gill, *Phys. Rev. Lett.* **103**, 123008 (2009).